Supplementary Information

Anion-mediated unusual enhancement of negative thermal expansion in the oxyfluoride of $PbTiO_3$

Zhao Pan,[a,b,*] Yue-Wen Fang,[c] Sergey A. Nikolaev,[b] Lin Wu,[d] Jie Zhang,[a] Mengqi Ye,[a] Jin Liu,[a] Xubin Ye,[a] Xiao Wang,[a] Takumi Nishikubo,[b,e] Yuki Sakai,[b,e] Runze Yu,[f] Shogo Kawaguchi,[g] Nianpeng Lu,[a] Yoshihiro Kuroiwa,[c] Jun Chen,[h,*] Masaki Azuma,[b,e,*] Xianran Xing,[h] and Youwen Long[a,i,*]

[a]*Beijing National Laboratory for Condensed Matter Physics, Institute of Physics, Chinese Academy of Sciences, Beijing, 100190, China*

[b]*Laboratory for Materials and Structures, Tokyo Institute of Technology, 4259 Nagatsuta, Midori, Yokohama, 226-8503, Japan*

[c]*Centro de F´ısica de Materiales (CFM-MPC), CSIC-UPV/EHU, Manuel de Lardizabal Pasealekua 5, 20018 Donostia/San Sebasti´an, Spain*

[d]*Graduate School of Advanced Science and Engineering, Hiroshima University, Higashihiroshima, Hiroshima 739-8526, Japan*

[e]*Kanagawa Institute of Industrial Science and Technology (KISTEC), 705-1 Shimoimaizumi, Ebina, Kanagawa 243-0435, Japan*

[f]*Center for High Pressure Science and Technology Advanced Research, Beijing 100193, PR China*

[g]*Research and Utilization Division, Japan Synchrotron Radiation Research Institute (JASRI), SPring-8, 1-1-1 Kouto, Sayo-cho, Sayo-gun, Hyōgo 679-5198, Japan*

[h]*Beijing Advanced Innovation Center for Materials Genome Engineering and Department of Physical Chemistry, University of Science and Technology Beijing, Beijing 100083, China*

[i]*Songshan Lake Materials Laboratory, Dongguan, Guangdong 523808, China*

*Corresponding author: zhaopan@iphy.ac.cn; junchen@ustb.edu.cn; mazuma@msl.titech.ac.jp; ywlong@iphy.ac.cn

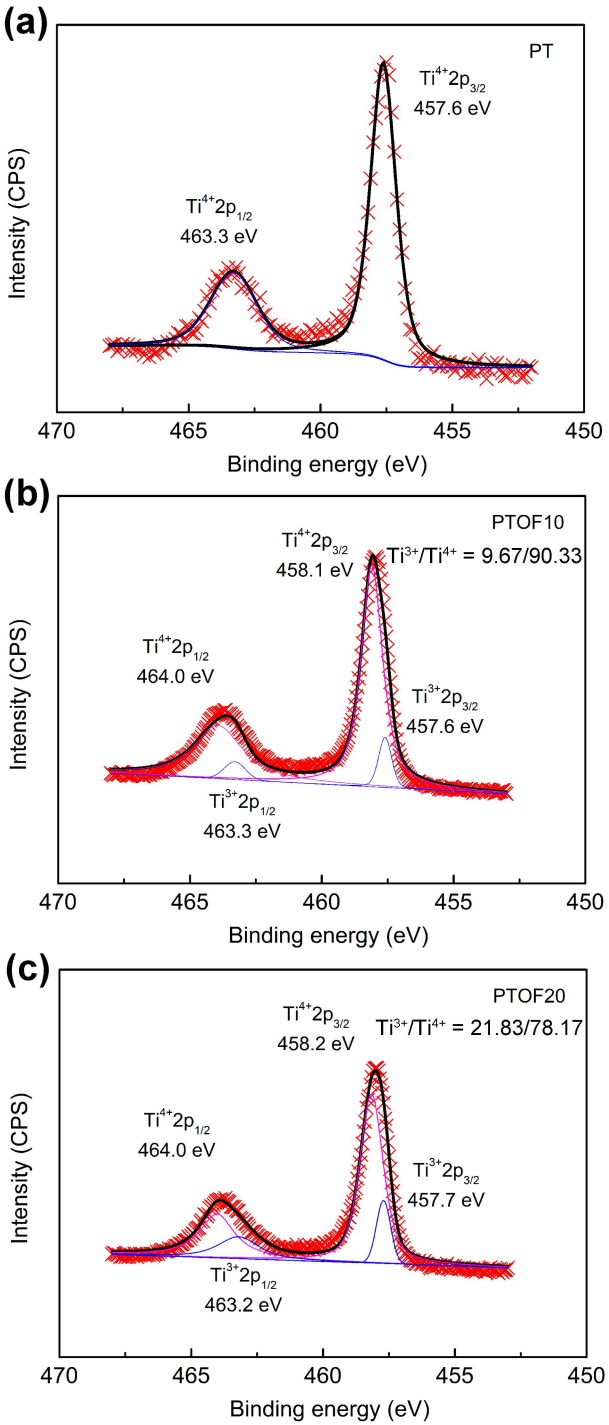

Fig. S1 X-ray photoelectron spectroscopy patterns (XPS) of Ti 2*p*. (a) $PbTiO_3$ (PT), (b) $PbTiO_{2.9}F_{0.1}$ (PTOF10), and (c) $PbTiO_{2.8}F_{0.2}$ (PTOF20).

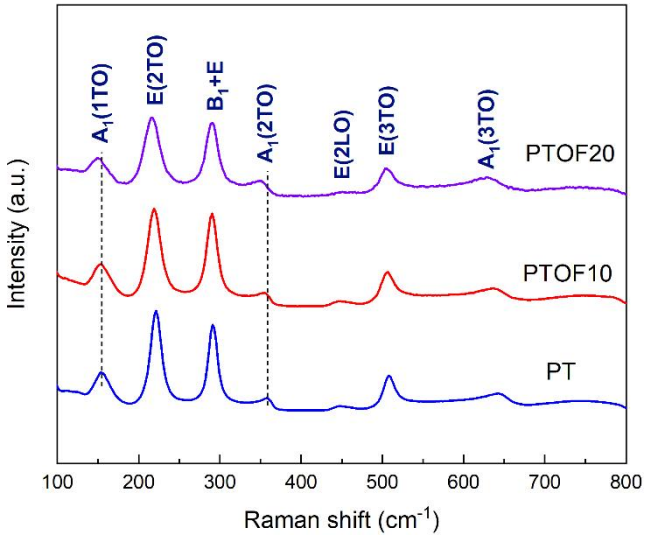

Fig. S2 Raman spectra of the PT, PTOF10, and PTOF20 compounds as a function of fluorine concentration at room temperature.

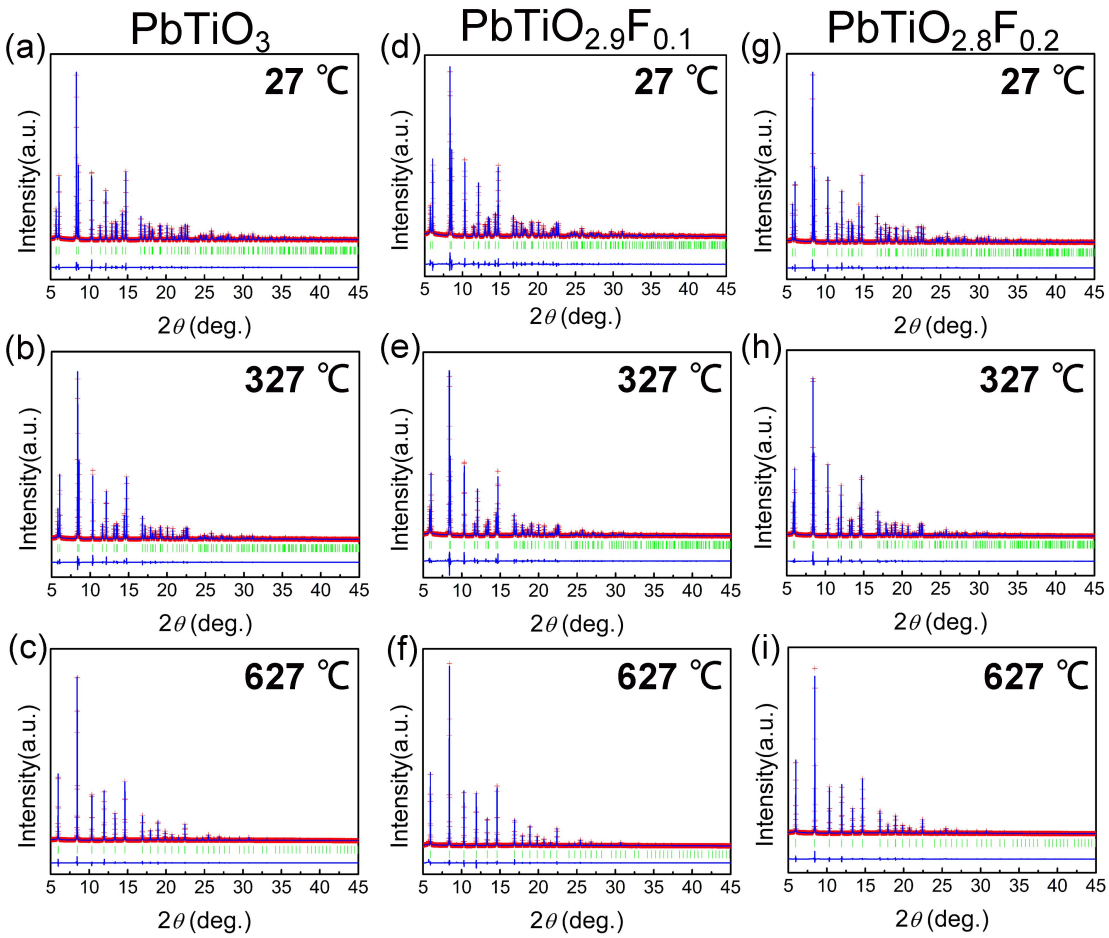

Fig. S3 Rietveld fitting patterns of synchrotron X-ray powder diffraction data in the tetragonal ferroelectric phase at room temperature ((a), (d), and (g)) and 327 °C ((b), (e), and (h)), and the cubic paraelectric phase at 627 °C ((c), (f), and (i)) of $PbTiO_3$, $PbTiO_{2.9}F_{0.1}$, and $PbTiO_{2.8}F_{0.2}$, respectively.

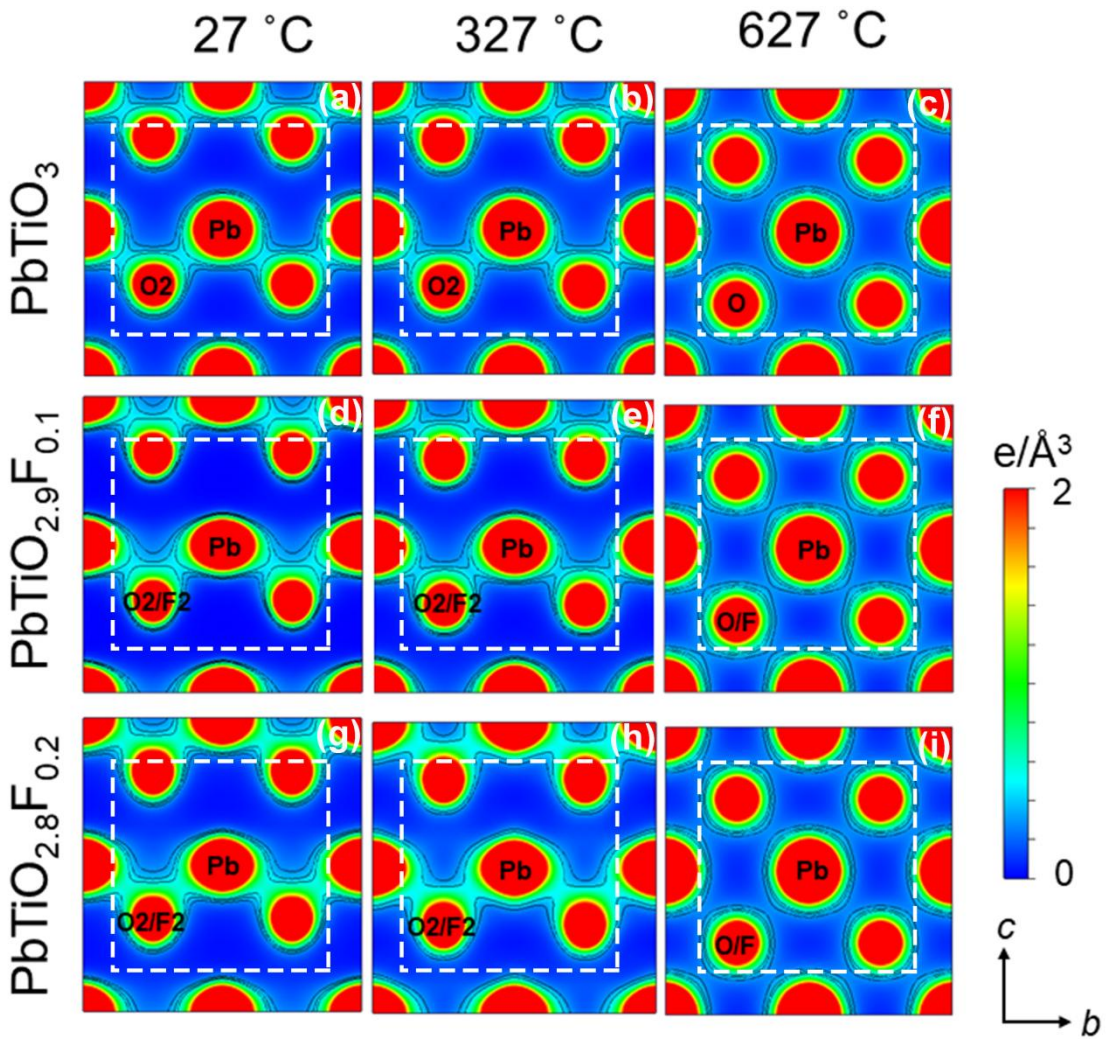

Fig. S4 Electron density distributions from the MEM calculations of $PbTiO_{3-x}F_x$ in the *bc* plane as a function of temperature in the tetragonal ferroelectric $PbTiO_3$ ((a) 27 ºC and (b) 327 ºC) and $PbTiO_{2.8}F_{0.2}$ ((d) 27 ºC and (e) 327 ºC) and cubic paraelectric $PbTiO_3$ ((c) 627 ºC) and $PbTiO_{2.8}F_{0.2}$ ((f) 627 ºC). Contours are shown from 0.3 to 0.6 $Å^{-3}$ by with interval of 0.1 $Å^{-3}$ in (a)-(i).

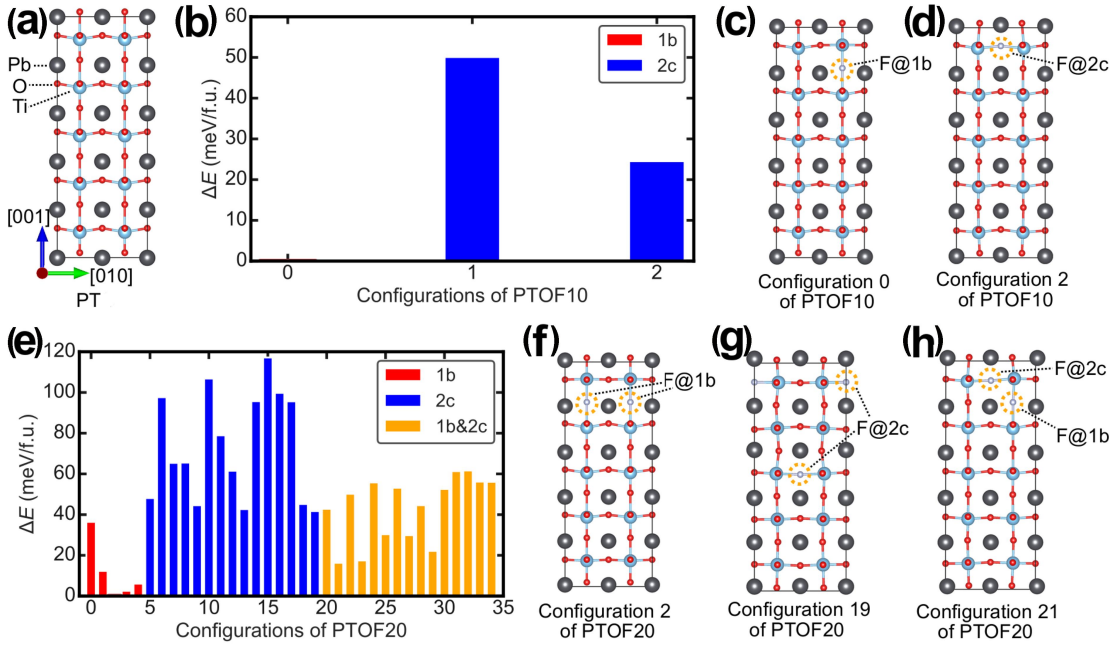

Fig. S5 First-principles calculations of $PbTiO_{3-x}F_x$ based on different configurations. (a) $1\times2\times5$ supercell of $PbTiO_3$ (PT). (b) Energy profile of $PbTiO_{2.9}F_{0.1}$ (PTOF10). (c) Configuration 0 of PTOF10 with the F dopant at the Wyckoff 1b site (F@1b). (d) Configuration 2 of PTOF10 with the F dopant at the Wyckoff 2c site (F@2c). (e) Energy profile of $PbTiO_{2.8}F_{0.2}$ (PTOF20). (f) Configuration 2 of PTOF20 with F@1b. (g) Configuration 19 of PTOF20 with F@2c. (h) Configuration 21 of PTOF20 with F@1b&2c.

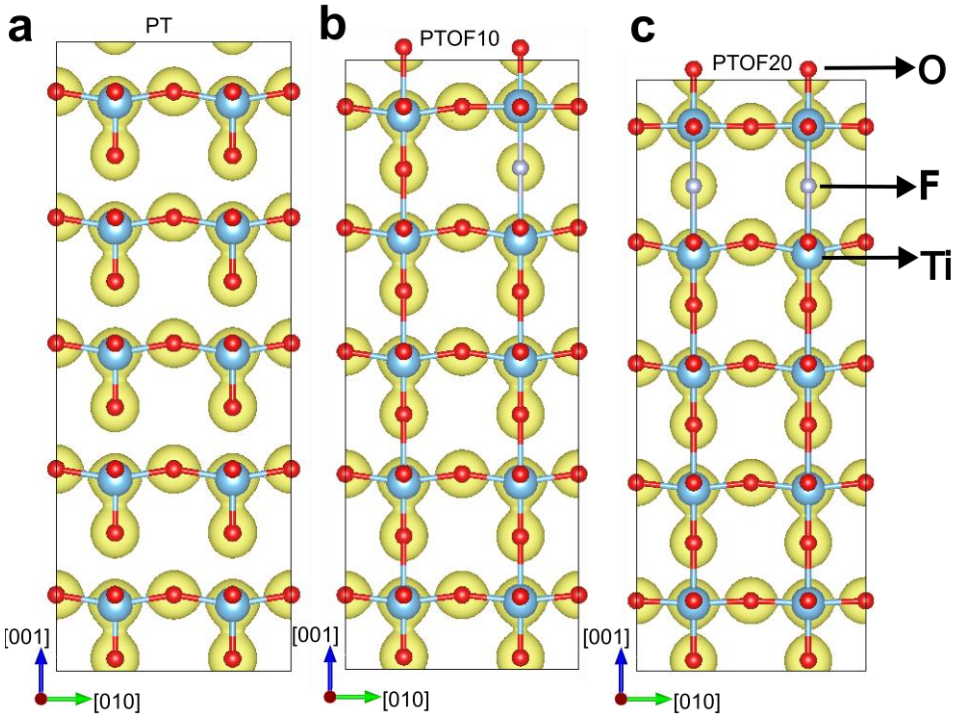

Fig. S6 The 3D charge density maps of (a) PTO, (b) PTOF10, and (c) PTOF20 projected onto the (100) plane.

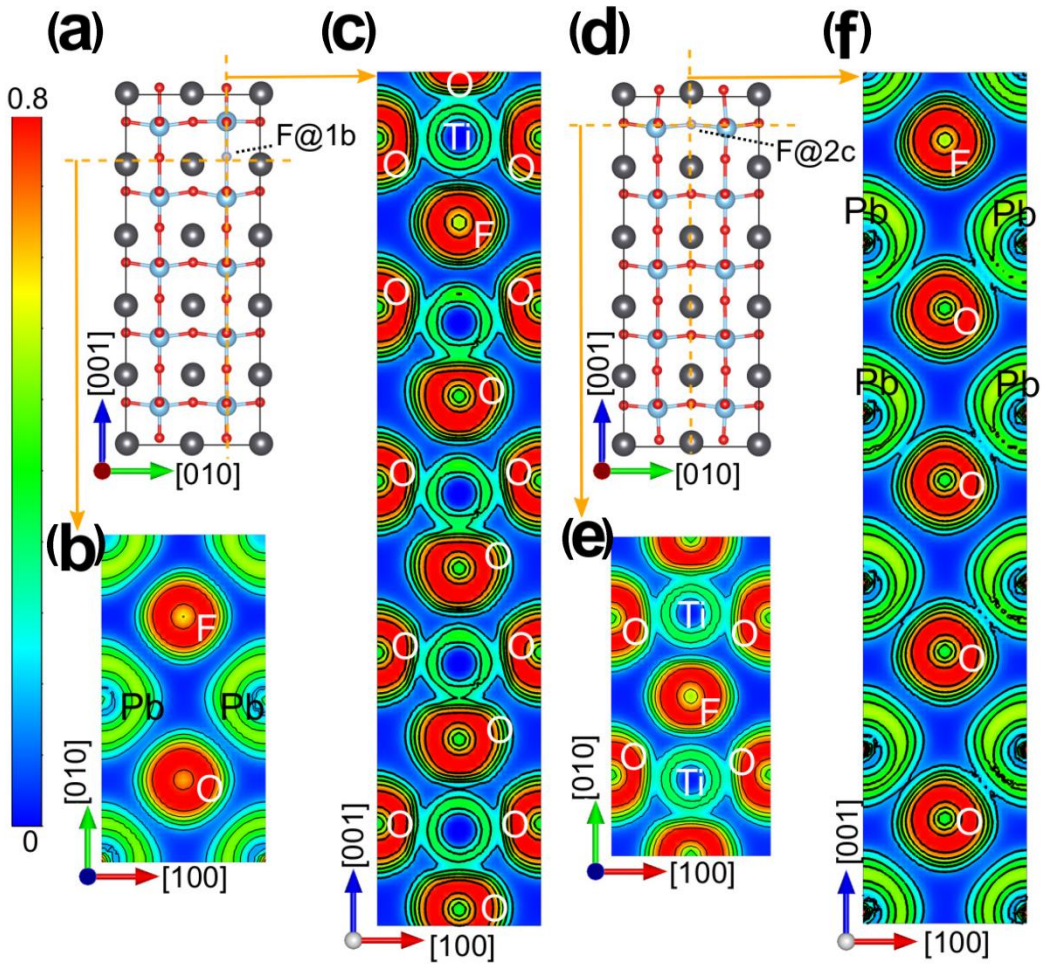

Fig. S7 Electron localization function for $PbTiO_{3-x}F_x$. (a) Configuration 0 of PTOF10 with F@1b and the corresponding ELF distribution in the (b) (001) and (c) (010) planes. (d) Configuration 2 of PTOF10 with F@2c and the corresponding ELF distribution in the (e) (001) and (f) (010) planes. The dashed orange lines in (a) and (d) show the projection planes, and the orange arrows are shown to guide the eyes.

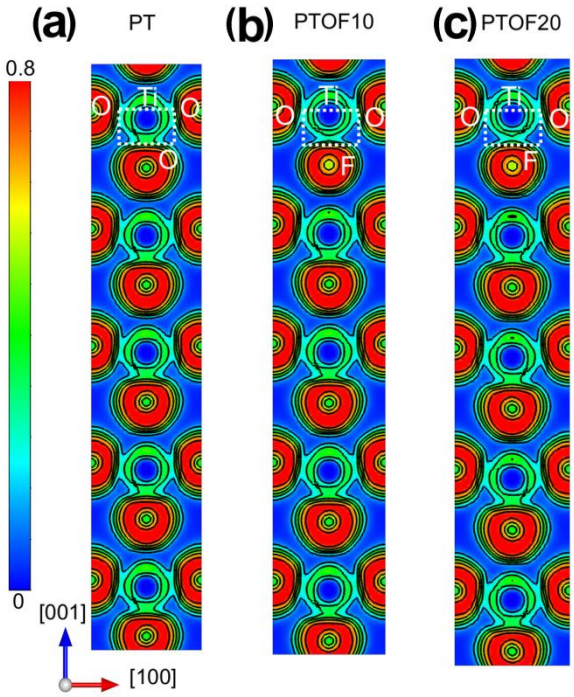

Fig. S8 ELF obtained for the experimental structures of (a) $PbTiO_3$ (PT), (b) $PbTiO_{2.9}F_{0.1}$ (PTOF10), and (c) $PbTiO_{2.8}F_{0.2}$ (PTOF20). The white dashed rectangles highlight the F doped Ti octahedra. The calculations were performed for the $1\times2\times5$ supercell, and the dopant positions correspond to the lowest energy configurations of the optimized structures.

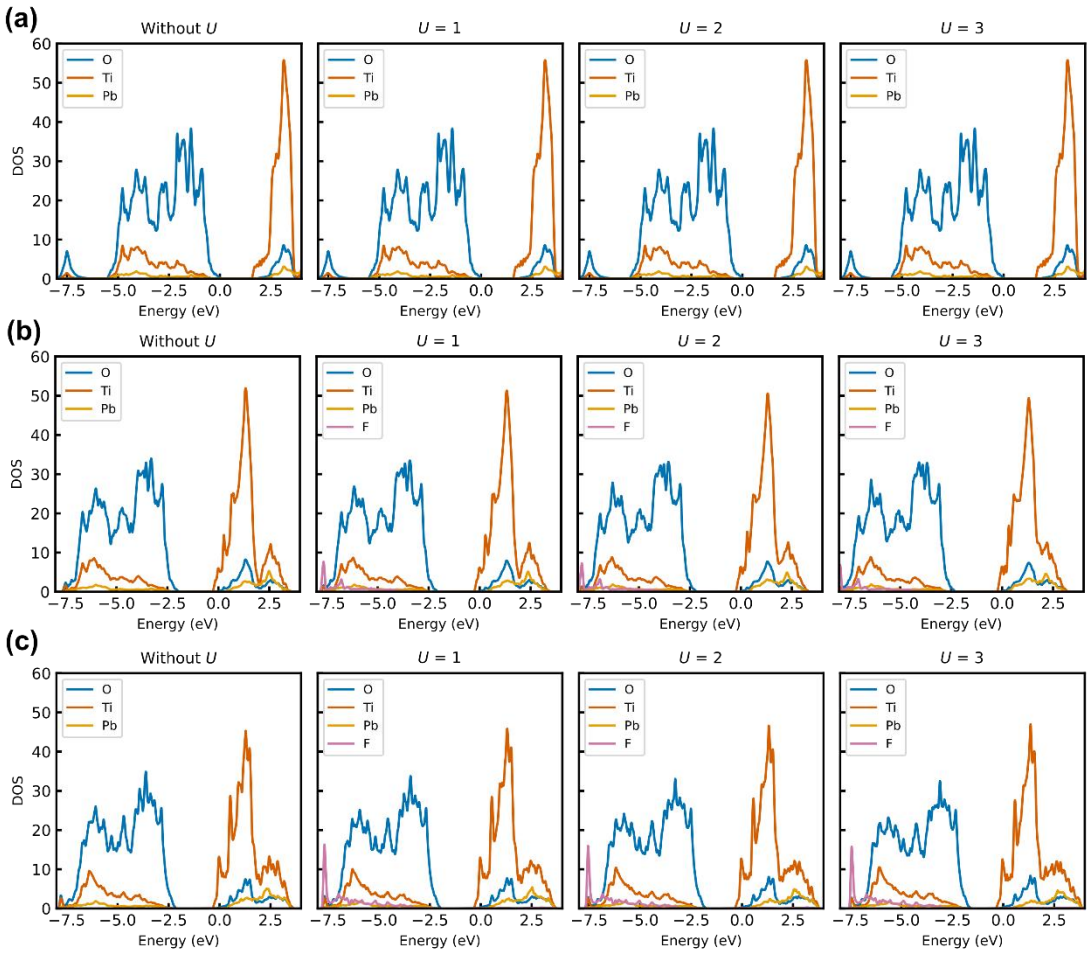

Fig. S9 Hubbard *U* effect on the density of states (DOS). (a) DOS of $PbTiO_3$. (b) DOS of $PbTiO_{2.9}O_{0.1}$. (c) DOS of $PbTiO_{2.8}O_{0.2}$.

Table SI. Crystal structure parameters obtained from first-principles calculations for undoped $PbTiO_3$ (PT) and the lowest energy configurations of $PbTiO_{2.9}F_{0.1}$ (PTOF10) and $PbTiO_{2.8}F_{0.2}$ (PTOF20). The structural data taken from the experiment is shown in brackets for a comparison.

Structural properties	Materials		
	PT	PTOF10	PTOF20
a [Å]	3.887 (3.901)	3.911 (3.906)	3.924 (3.908)
c [Å]	4.155 (4.150)	4.083(4.132)	4.044 (4.126)
V [Å^3]	62.777 (63.154)	62.453 (63.041)	62.269 (63.014)
c/a	1.069 (1.064)	1.044 (1.058)	1.031 (1.055)

Table SII. Average Bader (static) charges calculated for undoped $PbTiO_3$ (PT) and the lowest energy configurations of $PbTiO_{2.9}F_{0.1}$ (PTOF10) and $PbTiO_{2.8}F_{0.2}$ (PTOF20).

Element	Materials		
	PT	PTOF10	PTOF20
Pb [e]	1.36	1.36	1.36
Ti [e]	2.14	2.13	2.11
O [e]	-1.17	-1.18	-1.18
F [e]	–	-0.79	-0.8

Table SIII. Average polar displacements along the c axis obtained from first-principles calculations for undoped $PbTiO_3$ (PT) and the lowest energy configurations of $PbTiO_{2.9}F_{0.1}$ (PTOF10) and $PbTiO_{2.8}F_{0.2}$ (PTOF20). The structural data taken from experiment is shown in brackets for a comparison.

Displacements [Å]	Materials		
	PT	PTOF10	PTOF20
δ_{Pb}	0.44(0.49)	0.38(0.48)	0.34(0.46)
δ_{Ti}	0.32(0.33)	0.25(0.32)	0.18(0.31)

Table SIV. The interatomic distance of $PbTiO_3$ (PT), $PbTiO_{2.9}F_{0.1}$ (PTOF10), and $PbTiO_{2.8}F_{0.2}$ (PTOF20) compounds at room temperature.

Distance (Å)	PT	PTOF10	PTOF20
Ti-O1/F1 (short)	1.682(3)	1.752(9)	1.751(10)
Ti-O1/F1 (long)	2.468(3)	2.378(9)	2.372(10)
Ti-O2/F2 (×4)	1.9755(4)	1.9644(14)	1.9664(15)
Pb-O1/F1(×4)	2.8093(6)	2.7990(12)	2.7991(13)
Pb-O2/F2(×4)	2.5318(13)	2.596(8)	2.592(8)
Pb-O2'/F2'(×4)	3.1985(16)	3.110(10)	3.111(10)